Preliminary Development and Testing of an EPS-SG Microwave Sounder Proxy Data Generator Using the NOAA Microwave Integrated Retrieval System

Yong-Keun Lee, Quanhua Liu, Christopher Grassotti, Xingming Liang, Shuyan Liu, Yan Zhou, and Ming Fang

***Abstract*—The European Organisation for the Exploitation of Meteorological Satellites currently plans to launch Meteorological Operational Satellite Second Generation A1 (Metop-SG A1) with the microwave Sounder (MWS) instrument in 2023. MWS is a cross-track scanning passive microwave radiometer measuring in the range from 23.8 to 229 GHz, which is similar to the Advanced Technology Microwave Sounder (ATMS) on board the satellites in the Joint Polar Satellite System (JPSS) program. To confirm the capability of operational retrieval systems with MWS before its operational deployment, the prerequisites are to have the MWS simulated brightness temperatures and to apply them to a proper testbed. In this study, a preliminary version of MWS proxy data generator has been developed to provide the MWS simulated brightness temperature datasets and the Microwave Integrated Retrieval System (MiRS) is used as a testbed for an operational retrieval system. ATMS simulated brightness temperature datasets are also generated in the same way in which the MWS simulated brightness temperature datasets are generated in order to have a consistent comparison between MWS and ATMS results. MiRS was run with the MWS simulated inputs and the results are comparable to those of the MiRS ATMS experiments. MiRS MWS total precipitable water accuracy and precision are within most JPSS requirements. The change in channel characteristics from ATMS to MWS including the addition of temperature sounding channels at 53.2 and 53.9 GHz and the polarization change in channels 1 and 2 appear to slightly improve performance of MWS over land temperature and water vapor retrievals, respectively.**

Manuscript received July 29, 2020; revised October 18, 2020 and January 20, 2021; accepted February 22, 2021. Date of publication February 24, 2021; date of current version March 24, 2021. This work was supported in part by NOAA under NA19NES4320002 at the Cooperative Institute for Satellite and Earth System Studies at the University of Maryland/Earth System Science Interdisciplinary Center. *(Corresponding author: Yong-Keun Lee.)*

Yong-Keun Lee, Christopher Grassotti, and Xingming Liang are with the Cooperative Institute for Satellite and Earth System Studies, Earth System Science Interdisciplinary Center, University of Maryland, NOAA Center for Satellite Application and Research, National Environmental Satellite, Data, and Information Service, College Park, MD 20740 USA (e-mail: yong-keun.lee@noaa.gov; christopher.grassotti@noaa.gov; xingming.liang@noaa.gov).

Quanhua Liu is with the NOAA Center for Satellite Applications and Research, National Environmental Satellite, Data, and Information Service, College Park, MD 20740 USA (e-mail: quanhua.liu@noaa.gov).

Shuyan Liu is with the Cooperative Institute for Research in the Atmosphere, Colorado State University, NOAA Center for Satellite Application and Research, National Environmental Satellite, Data, and Information Service, College Park, MD 20740 USA (e-mail: shu-yan.liu@noaa.gov).

Yan Zhou is with the Cooperative Institute for Climate and Satellites-MD/Earth System Science Interdisciplinary Center, University of Maryland, College Park, MD 20740 USA (e-mail: yanzhou@umd.edu).

Ming Fang is with the I.M. Systems Group, NOAA Center for Satellite Application and Research, National Environmental Satellite, Data, and Information Service, College Park, MD 20740 USA (e-mail: ming.fang@noaa.gov).

Digital Object Identifier 10.1109/JSTARS.2021.3061946

***Index Terms*—Advanced Technology Microwave Sounder (ATMS), European Polar System—Second Generation (EPS-SG), Microwave Integrated Retrieval System (MiRS), microwave sounder.**

I. Introduction

THE European Organisation for the Exploitation of Meteorological Satellites (EUMETSAT) planned series of polar-orbiting satellites and associated space-borne instruments, known as the European Polar System—Second Generation (EPS-SG), is the follow on mission to its current Metop series. The series will deploy a number of earth-observing instruments ranging from passive imagers and sounders operating at microwave, infrared, and visible wavelengths, to radio occultation observing systems, as well as active microwave scatterometers [1]. Similar to the current Metop series, these satellites will fly in the mid-morning (local time) orbit, and will complement the data collection from the National Oceanic and Atmospheric Administration (NOAA) Joint Polar Satellite System (JPSS) series, which are situated in an early afternoon orbit. In this article, we report on development and testing of a proxy data simulator for the microwave sounder (MWS) instrument, scheduled to be aboard the first satellite of the EPS-SG series, Metop-SG A1, with a tentative launch date of 2023. A primary motivation for creation of a proxy data generator is that operational science algorithms, such as retrieval systems, need to be extended and tested in advance of operational deployment to ensure proper functioning with minimal issues once real data become available. Additionally, the simulated data can be used to address potential science questions, for example, the possibility of added information content provided by any new spectral channels not present on earlier operational satellite missions. Once proxy data have been generated, a proper testbed is needed to evaluate the retrieval performance and identify any potential issues. Since the geophysical "truth" data used to generate the simulated MWS data are known, a quantitative evaluation of retrieval algorithm performance can be conducted. Here, we use the NOAA Microwave Integrated Retrieval System (MiRS) as a testbed, which is the NOAA official microwave-only operational retrieval algorithm [2], [3].

The outline for this article is as follows. In Section II, we provide descriptions of the MWS and ATMS instruments, highlighting their similarities and differences. In Section III, we provide a general description of the MiRS algorithm. Section IV

TABLE I
ATMS AND MWS INSTRUMENT CHARACTERISTICS

Channel ATMS/ MWS	Central Freq. (GHz)	Bandwidth (MHz)	Pol.	Nadir FOV (km)
1/1	23.8	270	V/H	75/40
2/2	31.4	180	V/H	75/40
3/3	50.3	180	H/H	32/20
4	51.76	400	H	32
5/4	52.8	400	H/H	32/20
/5	53.246±0.08	2x140	/H	/20
6/6	53.596±0.115	2x170	H/H	32/20
/7	53.948±0.081	2x142	/H	/20
7/8	54.4	400	H/H	32/20
8/9	54.94	400	H/H	32/20
9/10	55.5	330	H/H	32/20
10/11	57.290344	2x155/330	H/H	32/20
11/12	57.290344±0.217	2x78	H/H	32/20
12/13	57.290344±0.3222±0.048	4x36	H/H	32/20
13/14	57.290344±0.3222±0.022	4x16	H/H	32/20
14/15	57.290344±0.3222±0.010	4x8	H/H	32/20
15/16	57.290344±0.3222±0.0045	4x3	H/H	32/20
16/17	88.2/89	2000/4000	V/V	32/17
17/18	164-167	2x1150 /2x1350	H/H	16/17
18/19	183.311±7.0	2x2000	H/V	16/17
19/20	183.311±4.5	2x2000	H/V	16/17
20/21	183.311±3.0	2x1000	H/V	16/17
21/22	183.311±1.8	2x1000	H/V	16/17
22/23	183.311±1.0	2x500	H/V	16/17
/24	229.0	2000	/V	/17

discusses the methodology used to generate the simulated MWS data. Section V contains retrieval impact results comparing simulated MWS with both simulated and real ATMS data retrievals. Finally, Section VI summarizes the overall results of this article.

II. INSTRUMENT DESCRIPTIONS

The ATMS and MWS sensors have many similarities but also contain significant differences. A summary of the instruments is shown in Table I. Both instruments are passive and cross-track scanning radiometers onboard the polar-orbiting satellite at about 825 km above Earth's surface. The channels sensitive to oxygen absorption between 50 and 60 GHz are used for atmospheric temperature sounding. The water vapor channel at 23.8 GHz and five water vapor channels around 183.31 GHz are for atmospheric moisture sounding. Channels at 23.8, 31.4, 89, and 165.5 GHz are important for inferring cloud, hydrometeor, and surface parameters. ATMS has 22 channels spanning 23.8 to 183.31 GHz [4], whereas MWS has 23 channels. In addition, MWS has a new channel at 229 GHz. The new channel at 229 GHz will provide higher sensitivity for the detection of cloud ice that affects channels from 89 to 183.31 GHz, and it can potentially improve the retrieval of light rain and snowfall rate. One of the significant differences between ATMS and MWS is the polarization configuration at nadir. As shown in Table I for the ATMS channels (black) and MWS channels (red after slash), ATMS channels 1 and 2 have quasi-vertical polarization, whereas MWS have quasi-horizontal polarization. For all five water vapor channels around 183.31 GHz, the two instruments have opposite polarization settings. The MWS has 95 scan positions with a maximum scan angle of 49.3°, which corresponds a swath of about 2100 km. The ATMS has 96 scan positions with a maximum scan angle of 52.725°, which corresponds a swath of about 2500 km. We do not include the specification values of NE Δ T because they are just the minimum requirement, and the ATMS actual performance in space is much better than the specification.

According to the EUMETSAT documentation, the footprint sizes of MWS channels 1 and 2 are significantly smaller by 47% at nadir than those of ATMS and the footprint sizes of MWS channels 3 to 16 are also smaller by 37% at nadir than those of ATMS [5]. From the remote sensing retrieval point of view, MWS with finer spatial resolution should provide more detailed surface features, water vapor, and cloud structure than by ATMS. From a data assimilation and modeling point of view, since numerical weather prediction (NWP) model grid spacing will be smaller when EPS-SG becomes available than when ATMS was launched, MWS with the smaller footprint sizes should provide more detailed information about atmospheric and surface spatial structure for NWP models.

The ATMS weighting functions for channels 1 to 3 and 5 to 15 [4] are the same as MWS channels 1 to 4 and 6, and 8 to 16 (black curves in Fig. 1 left panel). The ATMS channel 4 (red curve) weighting function peak is below the weighting peak of MWS channels 5 and 7 (cyan curves). For the right panel of Fig. 1, both ATMS channels 16 to 22 and MWS channels 17 to 23 have the same weighting functions (black curves). The MWS new channel 24 at 229 GHz (cyan curve) is sensitive to water vapor and ice clouds in the troposphere. We note that calculation of the weighting function using dz for the denominator, as is done here, may produce a different result if, instead, the denominator of $d(\log P)$ is used, since it depends on both dz and atmospheric layer temperature.

III. MICROWAVE INTEGRATED RETRIEVAL SYSTEM (MIRS) DESCRIPTION

The MiRS[1], has been NOAA's official operational microwave retrieval algorithm since 2007. Compared to visible and infrared radiation, microwaves have a longer wavelength, and thus can penetrate through the atmosphere more effectively. This feature allows microwave observations under almost all weather conditions including in cloudy and rainy atmospheres. MiRS follows a 1-D variational (1DVAR) methodology [2], [3]. The inversion is an iterative physical algorithm in which the fundamental physical attributes affecting the microwave observations are retrieved physically, including the profiles of atmospheric temperature, water vapor, nonprecipitating cloud, hydrometeors, as well as surface emissivity and skin temperature [6]. The Joint Center for Satellite Data Assimilation community radiative transfer model (CRTM) [7], [8] is used as the forward and Jacobian operator to simulate the radiances at each iteration prior to fitting the measurements to within the combined instrument and forward model noise level. After the core parameters of the state vector

[1]Online. [Available]: https://www.star.nesdis.noaa.gov/mirs

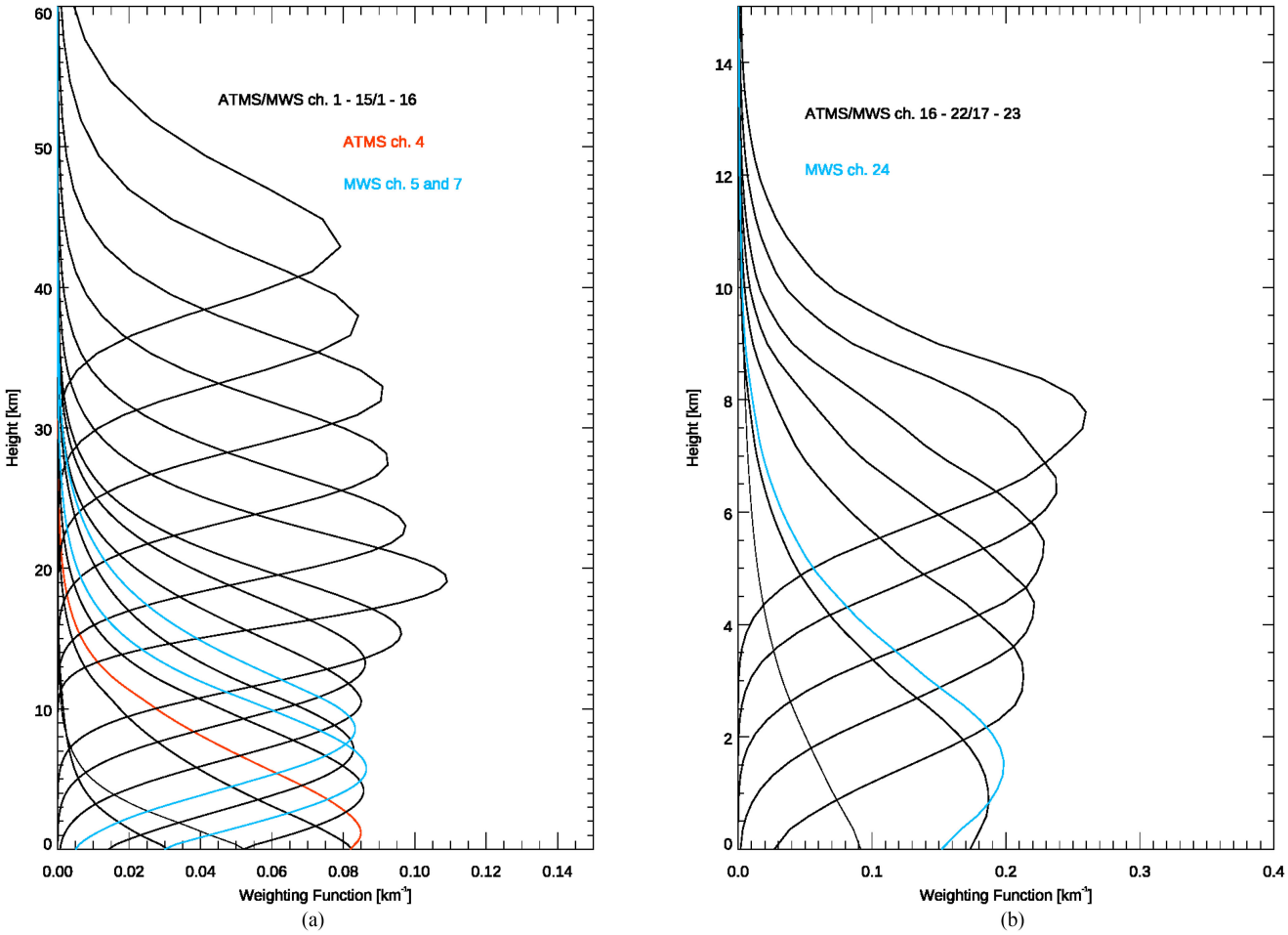

Fig. 1. ATMS and MWS weighting functions at nadir for U.S. standard atmosphere. Black curves show that the two instruments have the same weighting functions. Red curves represent the ATMS channels 4 and cyan curves are for MWS channels 5, 7, and 24. (a) Central frequencies lower than 60 GHz. (b) Central frequencies higher than 80 GHz.

are retrieved in the 1DVAR step, an additional postprocessing is performed to retrieve derived parameters based on inputs from the core 1DVAR retrieval. The postprocessing products include total precipitable water (TPW), snow water equivalent, snowfall rate, surface precipitation rate, etc. [9], [10]. A schematic of the MiRS processing components and data flow is shown in Fig. 2.

IV. Microwave Sounder (MWS) Proxy Data Simulator

Initially, one orbit of MWS proxy data was received from EUMETSAT, valid on September 12, 2007 and based on Metop-A measurements. Since the data, written in netCDF format, were in the expected official operational Level 1 format, this was primarily used to test input/output functionality within MiRS. Also NEdT values in their proxy data have been applied to the experiments in this study. However, the fact that the data were limited to a single orbit, and the original "truth" data used to generate it were not available limited its utility. In order to develop the MiRS system for MWS data processing, proxy data are required that cover different geographical regions and seasons for calculating *a priori* constraints, for example, the surface emissivity error covariance.

MiRS does retrieve the surface microwave emissivity with good variability over a range of surface types and in different seasons [6], but differences in polarizations and frequencies for some MWS channels (as noted in Section II and summarized in Table I) prevent us from using the *a priori* constraints from ATMS-based surface emissivity directly. Those surface-sensitive channels in which MWS polarization differs from ATMS are expected to have different emissivity characteristics, affecting both the mean spectrum as well as its covariance. Over oceans, we use the surface emissivity model FASTEM [11] in which polarization effects, as well as those due to frequency, incidence angle, wind speed, and salinity, are explicitly treated. In this article, for nonocean surfaces, we have developed a simple model to calculate MWS channel emissivity based on the MiRS retrieved surface emissivity.

The MiRS retrieved emissivity over land, ice, and snow surfaces is an operational environmental data record. The surface microwave emissivity depends on many parameters, such as surface roughness and dielectric constant, sensor scan angle, and channel central frequency. For a given location at a given time

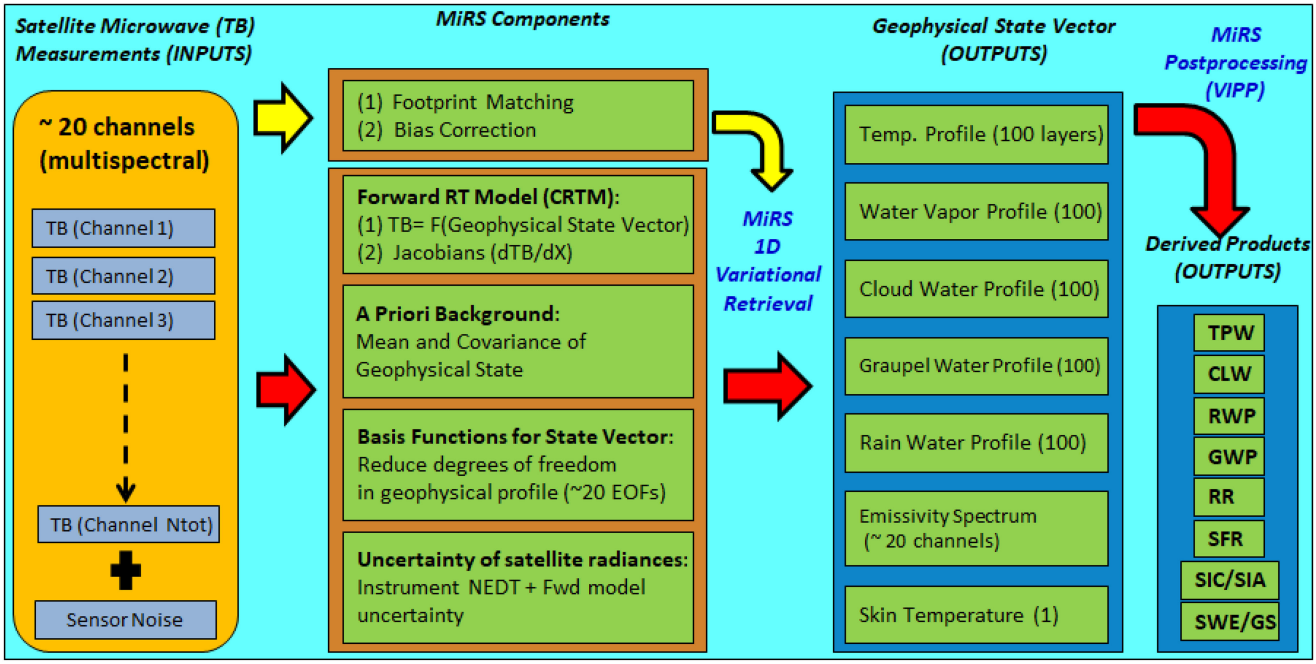

Fig. 2. Schematic of MiRS processing components and data flow showing MiRS core retrieval and postprocessing components. Core products are retrieved simultaneously as part of the state vector. Postprocessing products are derived through vertical integration. TB = brightness temperature; dTB/dX = Jacobian rate of change of brightness temperature with respect to a change in the geophysical state vector X; EOF = empirical orthogonal function, the basis functions used to represent the geophysical profile in the retrieval; NEDT = noise equivalent delta temperature; TPW = total precipitable water; CLW = cloud liquid water; RWP = rain water path; GWP = graupel water path; RR = rain rate; SFR = snowfall rate; SIC/SIA = sea ice concentration/sea ice age; and SWE/GS = snow water equivalent/snow grain size.

and a given channel (i.e., given surface roughness and dielectric constant) and a given scan angle, the surface emissivity may be written as a function of the channel central frequency f. Both ATMS and MWS are cross-scanning; therefore, for a given channel, its surface emissivity may be expressed as mixed pure vertically and horizontally polarized emissivity given by

$$\varepsilon = \epsilon_V \cos^2(\theta_{\text{scan}}) + \epsilon_H \sin^2(\theta_{\text{scan}}) \quad (1)$$

for a quasi-vertically (QV) polarized channel and

$$\varepsilon = \epsilon_V \sin^2(\theta_{\text{scan}}) + \epsilon_H \cos^2(\theta_{\text{scan}}) \quad (2)$$

for a quasi-horizontally (QH) polarized channel. We use a quadratic and inverse formulation to describe the dependence at a frequency f for pure vertical or horizontal polarization as

$$\epsilon_V = b_1 + b_2 \times f^{-1} + b_3 \times f^2 \quad (3)$$

and

$$\epsilon_H = b_4 + b_5 \times f^{-1} + b_6 \times f^2. \quad (4)$$

Therefore, for each individual field of view, we need to dynamically determine the six unknown coefficients b_i for each location at a given time. The predictors f^{-1} and f^2 are chosen for the consideration of inverse and quadratic variations based on our experimental results. This functional form allows for the variety of microwave spectra shapes found over most surfaces, for example, decreasing with frequency over scattering media, such as snow and ice, and increasing with frequency over land for frequencies less than 89 GHz. We can take six of MiRS retrieved emissivities at ATMS channels 1, 2, 3, 4, 16, and 17 (three QV and three QH), which allow for an exact solution of the six unknown coefficients. Once the coefficients are solved for in (3) and (4), (1) and (2) can be used to estimate the surface emissivity for MWS channels, depending on the polarization of the channel in question. Emissivities for frequencies higher than 165.5 GHz (ATMS channel 17) are extrapolated from the emissivities at the ATMS channels 16 and 17. Note that the fitting coefficients in (3) and (4) are calculated for each scan position and for every scan line. It is understood that the estimated surface emissivity is not truth and the estimation uncertainty can be transferred into the MWS proxy data. The purpose of the MWS proxy data is to obtain reasonably large dynamic ranges of the surface emissivities for calculating the surface emissivity error covariance matrix (required as an *a priori* constraint in the MiRS 1DVAR retrieval) and reasonable surface and weather features in the simulated brightness temperatures. Fig. 3 shows single-scene case studies for the ATMS surface emissivity (MiRS retrieved, black line) and MWS estimated surface emissivity (cyan line) spectra over ice, forest, and snow scenes. The scan angle is approximately 29°. As one can see, the ATMS and MWS surface emissivities between 50 and 165.5 GHz are practically the same because they share the same polarization and very similar frequency for those channels. The large differences are for channels 1 and 2 because of the opposite polarization. As noted, because of the difficulty of accurately estimating the emissivity at 183 GHz over most surfaces due to water vapor absorption, the values at this frequency were extrapolated from the emissivities at 89 and 165 GHz, meaning that the MWS emissivities reflect the quasi-horizontal polarization of ATMS rather than quasi-vertical

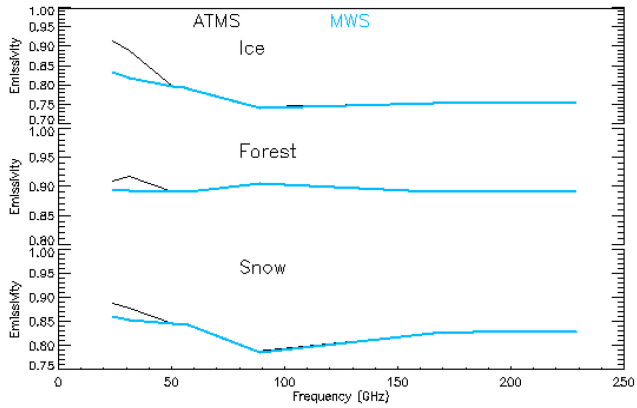

Fig. 3. ATMS (black line) and MWS (cyan line) surface emissivity over ice, forest, and snow. This is just one case. The snow and ice emissivities have large variabilities and can have different spectral behaviors.

polarization. Once real MWS data become available at 229 GHz, it will be possible to better estimate the emissivity at 183 GHz in clear areas as 229 GHz will be less affected by water vapor absorption.

Using the estimated MWS surface emissivity from (1) to (4) and the European Centre for Medium-Range Weather Forecasts (ECMWF) model variables of the atmosphere and surface, we can apply the CRTM to simulate the MWS brightness temperatures at the top of the atmosphere. In this preliminary version of the proxy data simulator, the CRTM cloud optical properties at 229 GHz are assumed to be the same as those at 183 GHz. Work is currently underway to extend the cloud properties to account for the increased sensitivity to ice cloud at 229 GHz, and once completed, the proxy data simulator will be updated to accommodate the change to CRTM.

For the MWS proxy data, the NOAA-20 ATMS orbital parameters are assumed. The swath width and scan positions are the same as ATMS, except for averaging ATMS two near nadir positions to a true nadir for the MWS. For the scan geometry, the first 47 fields of view (FOV) are the same for the ATMS and MWS. The MWS at nadir (MWS 48th FOV) is the mean position of ATMS FOVs at 48th and 49th scan positions. The MWS FOVs from 49 to 95 are the same as ATMS FOVs from 50 to 96. The MWS simulated data are written in a netCDF file that uses the same Level 1 format as EUMETSAT proxy data. In Fig. 4, the flowchart of the MWS proxy data simulator is provided.

V. Retrieval Assessments

There are two main issues with the MWS implementation on MiRS: first, how to generate static ancillary data adapted to MWS in the MiRS algorithm, and, second, how to measure the accuracy of the MiRS results using MWS proxy data. As noted, EUMETSAT provided one orbit of MWS proxy data; however, these data are insufficient for fully developing and testing an extension of MiRS to process MWS data. Therefore, NOAA/The Center for Satellite Applications and Research (STAR) generated 4 days of MWS simulated brightness temperature data based on NOAA-20 ATMS and the collocated ECMWF analysis

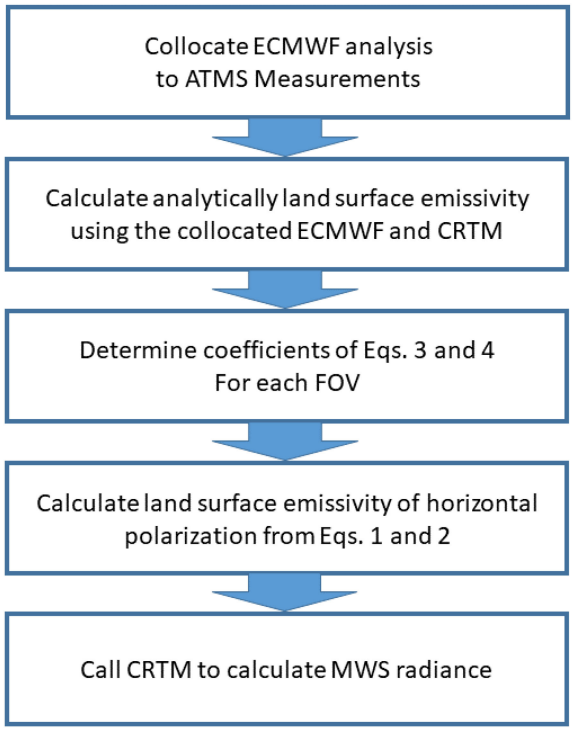

Fig. 4. Flowchart for the MWS proxy data simulator.

data with global coverage and spanning different seasons using the MWS proxy data simulator described in Section IV. Since one step in the simulator is the mapping of ATMS to MWS emissivities, by using these 4 days of MWS simulated data, static ancillary files (i.e., emissivity mean, covariance, and empirical orthogonal function basis functions) adapted to the MWS instrument could be generated offline. It is also important to determine the performance of the MiRS retrievals with the MWS simulated measurement data as inputs. The truth datasets in this study are the collocated ECMWF analysis data, which are mapped to each MWS field of view location. The collocation between ECMWF and ATMS is performed to find the spatially interpolated value of ECMWF variables from the four points in a latitude and longitude box and temporally interpolated between the two closest UTC hours out of 00, 06, 12, and 18 UTC. To run MiRS, the covariance matrix and EOF values of surface emissivity are needed. Therefore, NOAA/STAR generated covariance matrix and EOF values from four days (February 15, July 15, September 15, and December 15 in 2019) of MWS surface emissivity based on the MWS brightness temperature. Additionally, as the MWS simulated data are generated, the ATMS simulated data are likewise generated using NOAA-20 to provide for a consistent comparison between MWS and ATMS in MiRS. Finally, the ATMS real measured brightness temperature datasets are the official operational Level 1 data. Hereafter, reference to MiRS ATMS simulated (or proxy) indicates the MiRS retrieval results using the ATMS simulated (or proxy) brightness temperature and MiRS ATMS operational indicates the MiRS retrieval results using the real observed ATMS brightness temperatures.

In the results that follow, the MiRS MWS capability is compared to that of the MiRS ATMS operational and the MiRS

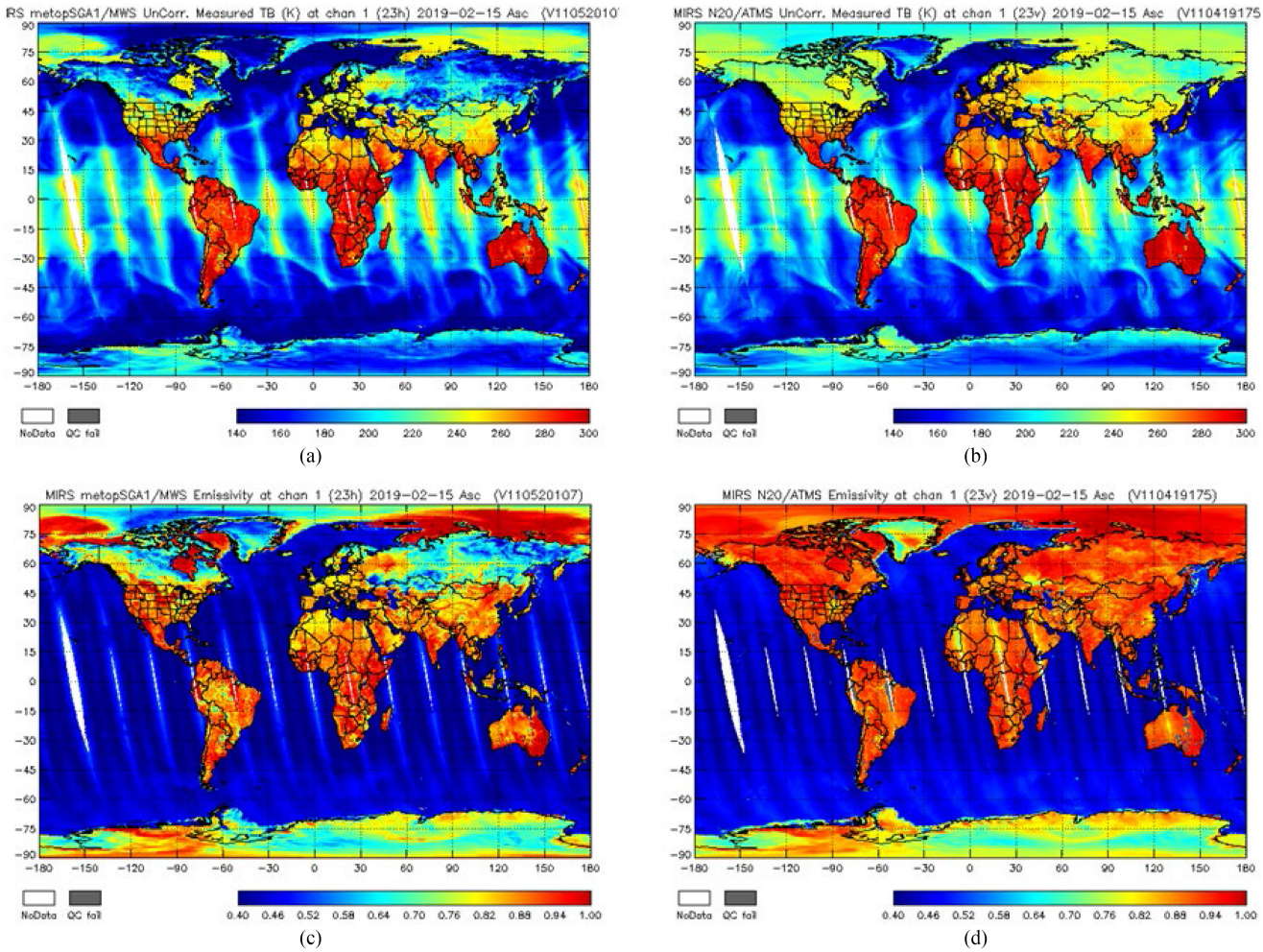

Fig. 5. (a) Simulated MWS and (b) real ATMS brightness temperatures (K) at 23.8 GHz, and (c) and (d) corresponding emissivities for ascending orbits valid on February 15, 2019.

ATMS simulated results. Since in CRTM, the cloud optical data base is not yet extended to 229 GHz (MWS channel 24), the 1DVAR retrieval procedure in MiRS excluded this channel in the inversion. Vertical temperature/moisture profiles, surface emissivity, and TPW are shown for the assessment of the MiRS MWS capability. In MiRS, vertical temperature/moisture profiles and surface emissivity are directly retrieved in the 1DVAR procedure, and TPW is one of the variables generated during the postprocessing step by simple vertical integration of the retrieved water vapor profile.

Fig. 5 shows simulated MWS and real ATMS brightness temperatures at 23.8 GHz (top panels) and corresponding retrieved emissivities (bottom panels) for ascending orbits valid on February 15, 2019. As discussed in Table I, MWS and ATMS polarizations at 23.8 GHz are quasi-horizontal and quasi-vertical, respectively, and thus the MWS brightness temperature at 23.8 GHz is generally less than that of ATMS globally. Therefore, as can be seen in Fig. 5(c)–(d), the retrieved MWS surface emissivity is generally lower than the ATMS emissivity at 23.8 GHz (consistent with Fig. 3). In particular, snow covered regions (northern America, Asia, and Europe) and sea ice (over the Arctic Ocean) are clearly distinguished by their different spectral signature in both brightness temperature and surface emissivity due to the polarization difference at 23.8 GHz.

Fig. 6(a)–(b) shows the vertical temperature profile standard deviation of the MiRS MWS simulated, ATMS simulated, and ATMS operational results compared to the collocated ECMWF analysis data under all sky conditions over sea and over land in ascending orbits on February 15, 2019 and August 25, 2020. Since the statistical difference between ascending and descending orbits is not significant, the results are shown only for ascending orbits. All sky conditions include clear, cloudy, and rainy. The number of samples for each case is approximately a few hundred thousand (not shown). The standard deviation values are between 1 and 2 K for the midtropospheric layers for all the retrievals on both days. In the troposphere below 400–600 hPa, the standard deviation values are larger over land than those over sea and near the surface the values increase to around or slightly over 2.5 K over land and up to around or slightly over 2 K over ocean. This is typically the case with microwave retrievals and is partly due to the fact that the land surface emissivity is generally larger and more highly variable than that at the sea surface. This

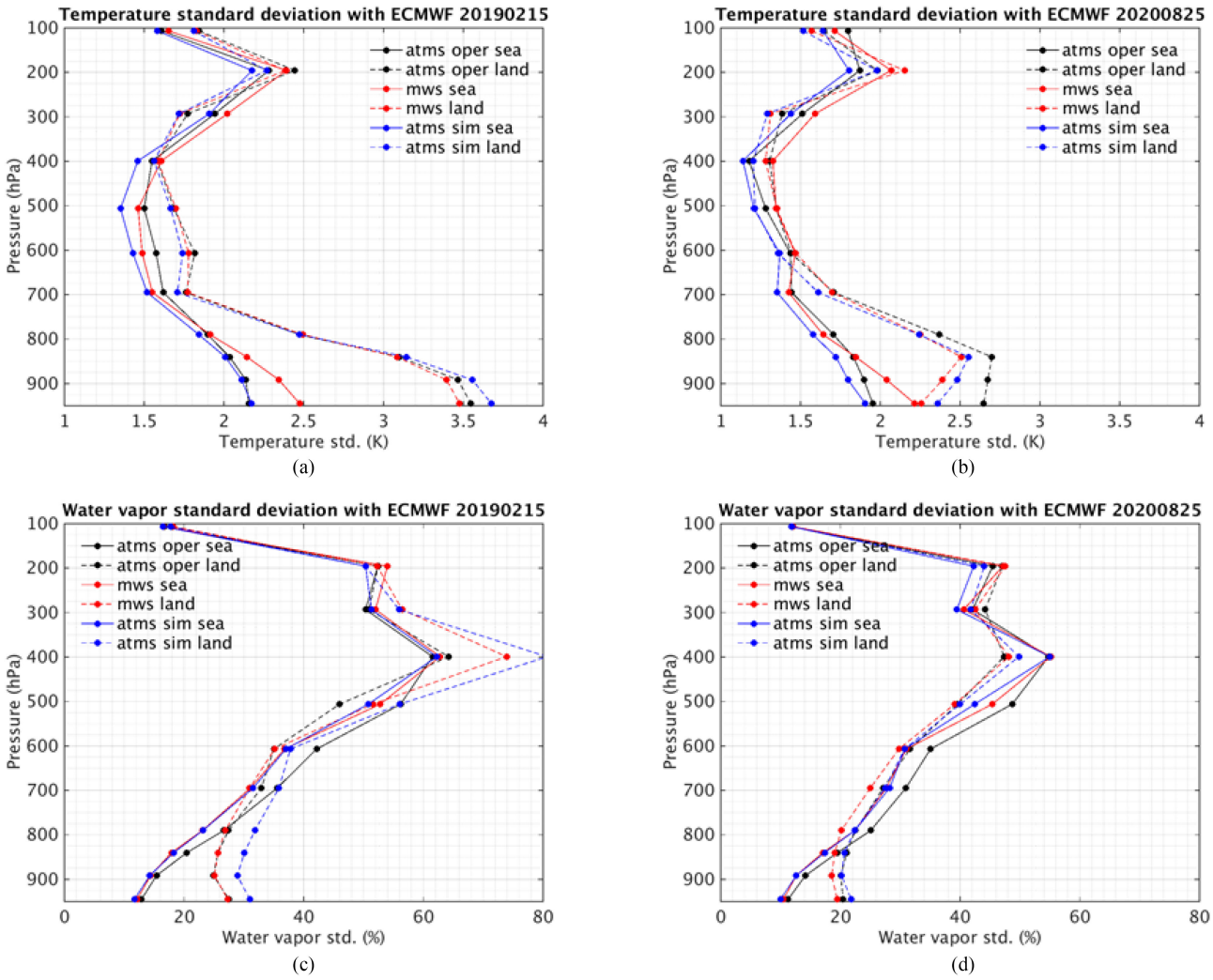

Fig. 6. Vertical temperature standard deviation (a) February 15, 2019 and (b) August 25, 2020 and vertical moisture standard deviation (c) February 15, 2019 and (d) August 25, 2020. The MiRS MWS simulated (red), the MiRS ATMS simulated (blue), and the MiRS ATMS operational retrievals (black) in ascending orbits. Thick lines are for sea and dotted lines are for land. Labeled experiments are as follows: ATMS oper sea: MiRS ATMS operational results compared to ECMWF analysis (over ocean); ATMS oper land: MiRS ATMS operational results compared to ECMWF analysis (over land); MWS sea: MiRS MWS results compared to ECMWF analysis (over ocean); MWS land: MiRS MWS results compared to ECMWF analysis (over land); ATMS sim sea: MiRS ATMS simulated results compared to ECMWF analysis (over ocean); ATMS sim land: MiRS ATMS simulated results compared to ECMWF analysis (over land).

increases the difficulty of detecting the signal of temperature and water vapor variations over land. The temperature profile standard deviation for MWS simulated results are comparable to ATMS experiment results, although over ocean in both February and August, MWS simulated retrieval performance appears slightly worse than simulated ATMS performance. Conversely, over land MWS temperature retrievals have slightly better performance in the lower troposphere. This may be due to the addition of two channels 5 and 7 on MWS at 53.2 and 53.9 GHz, which may provide additional information on atmospheric temperature over higher emissivity land near the surface. Fig. 6(c)–(d) shows the vertical water vapor profile statistics compared to the collocated ECMWF analysis data under all sky conditions where standard deviation is computed for (MiRS water vapor mixing ratio–ECMWF water vapor mixing ratio) and divided (or normalized) by the mean global ECMWF water vapor for each vertical layer multiplied by 100. The magnitude of standard deviation is generally similar between over land and over ocean at higher altitudes. The magnitude of standard deviation near the surface is larger over land than over sea similar to the temperature profile comparison in Fig. 6(a)–(b). MWS water vapor retrieval performance over land is better than the simulated ATMS performance, which may be related to the MWS use of horizontally polarized channels at 23.8 and 31 GHz, which allow more signal of water vapor variations to be detected over higher emissivity land surfaces. The results from both the vertical temperature and water vapor statistics highlight one of the main results of this article, which is because the MiRS MWS retrieval performs reasonably and comparably to the MiRS ATMS simulated and ATMS operational retrievals.

Fig. 7 shows the MiRS retrieved TPW results using the simulated MWS data and the ATMS real data. TPW is the integration of the retrieved water vapor amount in a given profile which weather forecasters often use to identify weather systems, such

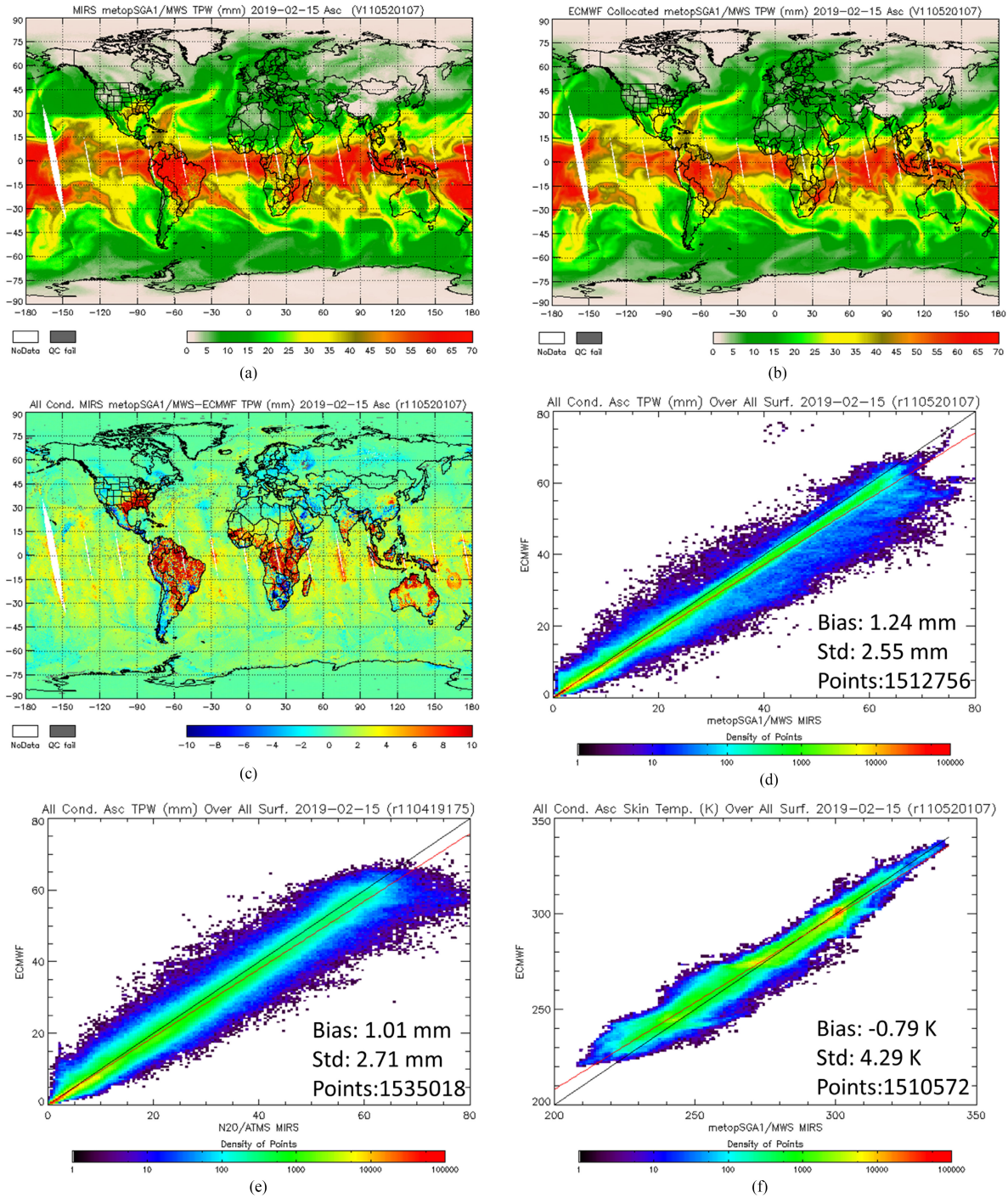

Fig. 7. Global TPW (mm) from (a) MiRS MWS retrieved and (b) collocated ECMWF analysis, (c) TPW difference (mm): MiRS MWS – ECMWF, (d) scatterplot between the MiRS MWS TPW and ECMWF TPW (density of points), (e) scatterplot between the MiRS ATMS operational TPW and ECMWF TPW (density of points), and (f) scatterplot between MiRS MWS skin temperature and ECMWF skin temperature (density of points) for ascending orbits February 15, 2019.

as fronts and atmospheric rivers, and to assess moistening or drying. Fig. 7(a) shows the MiRS retrieved TPW using simulated MWS data for ascending orbits, while Fig. 7(b) shows the global coverage of collocated ECMWF TPW at the same time. Generally high agreement is seen between the two maps. High TPW values are concentrated following the Intertropical Convergence Zone near the equator. Since it is in February, high TPW values are located at the South Pacific Convergence Zone from Southeast Asia to Southeast to French Polynesia and the Cook Islands. Several water vapor plumes are stretched to the midlatitudes where the rainfall is frequently observed. Fig. 7(c) is the TPW difference between the two estimates (MiRS MWS—ECMWF). Larger TPW differences are located in both tropical and the midlatitude areas; some of the TPW difference

TABLE II
TPW STATISTICS USING ECMWF ANALYSIS

Scene	Bias (mm)	Req.	Std. (mm)	Req.	# of FOVs 2019.02.15
			Sea		
Clear	1.53/2.20/1.60	1.5	1.26/1.41/2.31	2.5	1131228/829127/1094613
cloudy	0.98/1.11/0.97	0.5	1.15/1.42/2.29	2.5	672454/971298/679664
			Land		
Clear+Cloudy	2.08/0.82/0.87	2.5	4.94/5.23/4.96	5.5	447356/458113/458057
			Sea Ice		
Clear+Cloudy	0.06/0.22/0.19	2.0	0.57/0.79/1.05	2.0	236095/258428/286369
			Snow		
Clear+Cloudy	-0.02/0.01/0.21	2.0	0.72/0.88/0.85	2.0	587540/565006/588131

Scene	Bias (mm)	Req.	Std. (mm)	Req.	# of FOVs 2020.08.25
			Sea		
Clear	1.68/2.58/1.75	1.5	1.25/1.44/2.46	2.5	1132095/850530/1115534
cloudy	1.03/1.23/0.89	0.5	1.21/1.48/2.17	2.5	753613/975500/680990
			Land		
Clear+Cloudy	1.93/2.30/0.70	2.5	4.20/4.76/4.38	5.5	713459/716331/727827
			Sea Ice		
Clear+Cloudy	0.01/0.32/0.13	2.0	1.12/1.30/1.26	2.0	186871/263242/297065
			Snow		
Clear+Cloudy	0.19/0.29/0.33	2.0	0.57/0.89/0.95	2.0	290363/284834/287003

TPW statistics using ECMWF analysis data as a reference for the MiRS MWS simulated, ATMS simulated, and ATMS real operational retrievals are shown over four surface types with the JPSS requirements for each sky condition in combined (ascending and descending) orbits valid on February 15, 2019 (upper) and August 25, 2020 (lower). For a/b/c in bias and standard deviation, "a" designates the MiRS MWS simulated, "b" the MiRS ATMS simulated, and "c" the MiRS ATMS operational. Bias is calculated as MiRS—ECMWF. Note that clear and cloudy are separated over sea, while clear and cloudy are combined for the other surface types: land, sea ice, and snow.

values are comparatively larger over land than over sea which, in part, might be due to the more complicated land surface and specification of the *a priori* emissivity constraints. The TPW bias and standard deviation values are 1.24 and 2.55 mm, respectively, under all sky conditions (clear, cloudy, and rainy) and all surface types (sea, sea ice, land, and snow) as shown in Fig. 7(d). The corresponding statistics of the MiRS ATMS operational TPW bias (MiRS ATMS operational—ECMWF) and standard deviation values are 1.01 and 2.71 mm, respectively in Fig. 7(e), showing consistency between the MWS and ATMS retrievals. The scatterplot for skin temperature between MiRS MWS and the ECMWF analysis in Fig. 7(f) shows that the bias is –0.79 K and the standard deviation is 4.29 K for all sky conditions and all surface types. Over land, the bias is 0.09 K and the standard deviation is 3.02 K (not shown), which well meets the JPSS requirement [12].

Table II shows TPW statistics for the MiRS MWS simulated, ATMS simulated, and ATMS operational for clear and cloudy skies over land, sea, sea ice, and snow, along with the corresponding JPSS program requirements [12] for combined orbits (ascending and descending) on February 15, 2019 and August 25, 2020. Clear and cloudy conditions are separated over sea while clear and cloudy are combined for other surfaces. The bias and standard deviation values of TPW from the MiRS MWS simulated sometimes are marginal (e.g., clear sea bias), however, mostly within the JPSS requirements, and are comparable to those from the MiRS ATMS simulated and the MiRS ATMS operational retrievals. Since TPW is the vertical integration of layer water vapor, there is a correlation of TPW statistics with the results for the vertical water vapor profile comparison with ECMWF analysis data. For example, on February 15, 2019, the water vapor bias from the MiRS MWS simulated retrieval shows positive values for all the vertical layers below 400 hPa over land (not shown) and the TPW bias is also positive for all cases. At the same time, the MiRS ATMS simulated and the MiRS ATMS operational retrievals show some negative values in the midtroposphere leading to a smaller overall TPW bias when compared to the simulated MWS results (not shown).

VI. CONCLUSION

EUMETSAT plans for the EPS-SG satellite series currently call for an initial launch of the Metop-SG A1 satellite in 2023

with the entire series lifetime of 25 years. Among the instruments to be on board, the A1 satellite is the MWS. In this study, we report on the preliminary development and testing of a proxy data simulator for the MWS instrument. The purpose of the simulator and the associated proxy data is to aid in the development, tuning, and testing of operational science algorithms and data processing systems prior to launch. MiRS was used as a testbed for the MWS simulated data in this study. To implement MWS capability within MiRS, any instrument-specific references and datasets need to be updated and extended. This includes required static ancillary datasets, such as surface emissivity mean, covariance matrix, and EOF basis values appropriate for the MWS frequencies and polarizations. Since ATMS and MWS have similar channels in terms of frequency but with different polarizations at some frequencies, the MiRS NOAA-20 ATMS retrieved surface emissivities are converted to those of MWS channels using a simple quadratic and inverse form in frequency. Then, the current MiRS NOAA-20 ATMS outputs and the collocated ECMWF analysis data are used as inputs for the simulator to generate MWS simulated brightness temperatures. Four days of the MWS simulated data are generated through the proxy data simulator to prepare the static ancillary datasets covering the global geography (in particular, varying surface types with different emissivity characteristics) and varying seasons. Similarly, ATMS simulated data were generated in the same way as the MWS data for a consistent comparison. The ECMWF analysis data are the reference in this study and the statistics of the MiRS MWS simulated against ECMWF are compared to that of the MiRS ATMS simulated (and operational) against ECMWF. MiRS was run end-to-end using the MWS simulated data following the same MiRS operational procedure as for Suomi National Polar-orbiting Partnership/NOAA-20 ATMS and Metop-A/B/C Advanced Microwave Sounding Unit-A and Microwave Humidity Sounding. The performance of the MiRS MWS simulated retrievals to ECMWF analysis data is comparable to that of the MiRS ATMS simulated and the MiRS ATMS operational retrievals. The MWS proxy data simulator will allow for continued testing, tuning, and validation of the MiRS retrieval system prior to actual launch and deployment of the instrument. Once the MWS instrument is deployed operationally, a proper radiometric bias correction specific to the instrument will be developed and applied to the MiRS retrieval to reduce the impact of systematic differences between the observed and CRTM simulated MWS radiances. Additionally, the effect of the channel 229 GHz in the MiRS retrieval will be investigated as soon as the CRTM cloud database incorporates this frequency.

ACKNOWLEDGMENT

The authors would like to thank EUMETSAT for the proxy data and NOAA Office of Project, Planning and Analysis (OPPA) for funding. The manuscript contents are solely the opinions of the authors and do not constitute a statement of policy, decision, or position on behalf of NOAA, or the U.S. Government.

REFERENCES

[1] V. Mattioli *et al.*, "The EUMETSAT polar systems Second generation (EPS-SG) passive microwave and Sub-mm wave missions," in *Proc. 41st Photon. Electromagn. Res. Symp.–Spring*, Jun. 2019, pp. 3926–3933.

[2] S. A. Boukabara *et al.*, "MiRS: An all-weather 1DVAR satellite data assimilation and retrieval system," *IEEE Trans. Geosci. Remote Sens.*, vol. 49, no. 9, pp. 3249–3272, Sep. 2011.

[3] S. A. Boukabara *et al.*, "A physical approach for a simultaneous retrieval of sounding, surface, hydrometeor, and cryospheric parameters from SNPP/ATMS," *J. Geophys. Res., Atmos.*, vol. 118, no. 22, pp. 12600–12619, 2013.

[4] Q. Liu and S. Boukabara, "Community radiation transfer model (CRTM) applications in supporting the Suomi National Polar-Orbiting Partnership (SNPP) mission validation and verification," *Remote Sen. Environ.*, vol. 140, pp. 744–754, 2014.

[5] MWS Science Advisory Group. "EPS-SG MicroWave Sounder (MWS) Science Plan," 2019. [Online]. Available: massif.eumetsat.int

[6] S. A. Boukabara, K. Garrett, and C. Grassotti, "Dynamic inversion of global surface microwave emissivity using a 1DVAR approach," *Remote Sens.*, vol. 10, no. 5, pp. 679–696, 2018.

[7] Y. Han *et al.*, "Community radiative transfer model (CRTM) - Version 1," National Oceanic and Atmospheric Administration, Washington, DC, USA, NOAA Tech. Rep. 122, pp. 33, 2006.

[8] S. Ding *et al.*, "Validation of the community radiative transfer model," *J. Quant. Spectrosc. Radiative Transf.*, vol. 112, no. 6, pp. 1050–1064, 2011.

[9] S. Liu, C. Grassotti, J. Chen, and Q. Liu, "GPM products from the microwave-integrated retrieval system," *IEEE J. Sel. Top. Appl. Earth Observ. Remote Sens.*, vol. 10, no. 6, pp. 2565–2574, Jun. 2017.

[10] S. Liu *et al.*, "The NOAA microwave integrated retrieval system (MiRS): Validation of precipitation from multiple polar orbiting satellites," *IEEE J. Sel. Top. Appl. Earth Observ. Remote Sens.*, vol. 13, no. 6, pp. 3019–3031, 2020.

[11] Q. Liu, F. Weng, and S. English, "An improved fast microwave water emissivity model," *IEEE Trans. Geosci. Remote Sens.*, vol. 49, no. 4, pp. 1238–1250, Apr. 2011.

[12] GSFC JPSS CMO, "Joint polar satellite system (JPSS) level 1 requirements document supplement (L1RDS) – final, JPSS-REQ-1002/470-00032, revision 2.11 joint polar satellite system (JPSS) code 472," Goddard Space Flight Center, Greenbelt, MD, USA, 2019, [Online]. Available: https://www.jpss.noaa.gov/assets/pdfs/technical_documents/L1RDS.pdf

Yong-Keun Lee received the B.S. and the M.S. degrees in atmospheric science from Seoul National University, Seoul, South Korea, in 1994 and 1996, respectively, and the Ph.D. degree in atmospheric science from Texas A&M University, College Station, TX, USA, in 2006.

From 2006 to 2018, he was with the Space Science and Engineering Center, University of Wisconsin, Madison, WI, USA. Since 2018, he has been with the Earth System Science Interdisciplinary Center, University of Maryland, College Park, MD, USA, and the National Oceanic and Atmospheric Administration, NOAA Center for Satellite Application and Research, National Environmental Satellites, Data, and Information Service, College Park, MD, USA.

Quanhua Liu received the B.S. degree in physics from Nanjing University of Information Science and Technology (formerly Nanjing Institute of Meteorology), Nanjing, China, in 1982, the M.Sc. degree in physics from the Chinese Academy of Science, Beijing, China, in 1984, and the Ph.D. degree in meteorology and remote sensing from the University of Kiel, Kiel, Germany, in 1991.

He is currently a Physical Scientist with the National Oceanic and Atmospheric Administration, National Environmental Satellite, Data, and Information Service, College Park, MD, USA, and leading the teams of Advanced Technology Microwave Sounder radiance calibration and Microwave Integrated Retrieval System projects. He contributes to the development of the community radiative transfer model (CRTM). The CRTM has been operationally supporting satellite radiance assimilation for weather forecasting. The CRTM also supports JPSS/NPP and GOES-R missions for instrument calibration, validation, long-term trend monitoring, and satellite retrieved products.

Christopher Grassotti received the B.S. degree in earth and space science from the State University of New York at Stony Brook, Stony Brook, NY, USA, in 1982, the M.S. in meteorology from the University of Wisconsin-Madison, Madison, WI, USA, in 1986, and the M.S. degree in viticulture and enology from AgroMontpellier, Montpellier, France, in 2007.

From 1986 to 1991 and again from 1993 to 2005, he was a Research Associate and Senior Research Associate with Atmospheric and Environmental Research, Inc., Lexington, MA, USA. From 1991 to 1993, he was with the Atmospheric Environmental Service, Environment Canada, Dorval, QC, Canada. Since 2008, he has been with the National Oceanic and Atmospheric Administration, NOAA Center for Satellite Application and Research, National Environmental Satellite, Data, and Information Service, College Park, MD, USA.

Xingming Liang received the B.S. degree in construction machinery from Jilin University, Changchun, China, the M.S. degree in information science, and the Ph.D. degree in remote sensing and atmospheric sciences at Saga University, Saga, Japan in 2002 and 2005, respectively.

He was a Research Scientist with the Cooperative Institute for Research in the Atmosphere, Colorado State University, Fort Collins, CO, USA from 2007 to 2016, and was a Senior Scientist with ERT, Inc., and GST, Inc., from 2016 to 2019. He is currently an Assistant Research Scientist with the Cooperative Institute for Satellite Earth System Studies, University of Maryland, College Park, MD, USA., and work at the Center for Satellite Applications and Research (STAR) of NOAA/NESDIS to develop the Artificial intelligence applications in remote sensing, and support the development of the Microwave Integrated Retrieval System (MiRS) and the community radiative transfer model (CRTM).

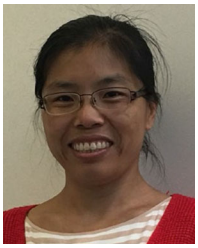

Shuyan Liu received the B.S. and M.S. degrees in atmospheric physics and environment from Nanjing Institute of Meteorology, Nanjing, China, in 2000 and 2003, respectively, and the Ph.D. degree in meteorology from Nanjing University of Information Science and Technology, Nanjing, China, in 2006.

From 2007 to 2011, she was a Model Developer with Illinois State Water Survey, University of Illinois at Urbana-Champaign, Champaign, IL, USA. From 2011 to 2015, she was with Earth System Science Interdisciplinary Center, University of Maryland, College Park, MD, USA. Since 2015, she has been with the Cooperative Institute for Research in the Atmosphere, Colorado State University, Fort Collins, CO, USA, and the NOAA Center for Satellite Application and Research, National Environmental Satellite, Data, and Information Service, College Park, MD, USA.

Yan Zhou received the B.S. degree in the major of atmospheric science from Zhejiang University, Hangzhou, China, in 2006, the M.S. degree in the major of atmospheric science from the University of Georgia, Athens, GA, USA, in 2008, and the Ph.D. degree in the major of atmospheric science from the University of Maryland, College Park, MD, USA, in 2014.

From 2015 to 2018, she was with the CICS-MD Observing System Simulation Experiment Project at the Earth System Science Interdisciplinary Center (ESSIC), University of Maryland. Since 2019, she has been with the ESSIC, in cooperation with NOAA Center for Satellite Applications and Research (NOAA/STAR), College Park, MD, USA, working on the Microwave Integrated Retrieval System (MiRS) Project.

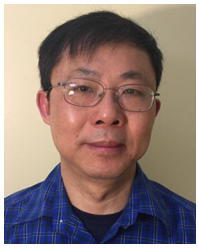

Ming Fang received the B.S. degree in atmospheric physics from the Nanjing University of Information Science and Technology (formerly Nanjing Institute of Meteorology), Nanjing, China, in 1983, and the M.Sc. and Ph.D. degrees in meteorology from the University of Oklahoma, Norman, OK, USA, in 2005 and 2008, respectively.

From 2006 to 2009, he was a Research Associate with the Cooperative Institution for Mesoscale Meteorological Studies, University of Oklahoma. From 2009 to 2017, he was an Associate Research Scientist with the Rosenstiel School of Marine and Atmospheric Science, University of Miami, Coral, Gables, FL, USA. From 2017 to 2019, he was a Senior Scientist with Aviation Meteorology Division, I.M. Systems Group, Inc., Rockville, MD, USA. Since 2019, he has been with I.M. Systems Group, Inc., and the National Oceanic and Atmospheric Administration, NOAA Center for Satellite Applications and Research, National Environmental Satellite, Data, and Information Service, College Park, MD, USA.